Nuclear Materials and Energy 12 (2017) 302–306

Contents lists available at ScienceDirect

Nuclear Materials and Energy

journal homepage: www.elsevier.com/locate/nme

The microstructure of tungsten exposed to D plasma with different impurities

M. Rasinski[a,*], A. Kreter[a], Y. Torikai[b], Ch. Linsmeier[a]

[a] Forschungszentrum Jülich GmbH, Institut für Energie- und Klimaforschung – Plasmaphysik, Partner of the Trilateral Euregio Cluster (TEC), 52425 Jülich, Germany

[b] Hydrogen Isotope Research Center, University of Toyama, Toyama 930-8555, Japan

ARTICLE INFO

Article history:
Received 15 July 2016
Revised 12 October 2016
Accepted 1 November 2016
Available online 17 November 2016

Keywords:
Mixed plasma
Impurity seeding
ELM mitigation
Divertor
Tungsten surface morphology

ABSTRACT

In this study the effect of impurities in deuterium plasma on the tungsten microstructure is investigated. W samples were exposed in the linear plasma generator PSI-2 at a sample temperature of 500 K with an incident ion flux of about 10^{22} $m^{-2}s^{-1}$, an incident ion fluence of 5×10^{25} m^{-2} and an incident ion energy of 70 eV. Samples were exposed to pure D+ plasma and with additional impurities of He (3%), Ar (7%), Ne (10%) or N (5%). After the PSI-2 exposure a part of each sample was additionally loaded with tritium to measure the tritium uptake using the imaging plate technique.

The surface morphology was investigated using scanning electron microscope (SEM) combined with a focused ion beam (FIB) utilized for cross-sectioning and thin lamella preparation for the transmission electron microscope (TEM) analysis.

Blistering with grain orientation dependence was observed on all exposed samples. Most pronounced blistering is reported for grains with orientation close to (111). The addition of Ar or Ne results in surface erosion with different yields depending on grain orientation. Highest erosion yield is observed for grains with orientation close to (100). Large blisters are present but show signatures of erosion. Less pronounced erosion is visible when adding N. The highest uptake of tritium was reported for the sample exposed to D+He plasma which corresponds to the largest – 18 nm, near surface damage zone revealed by TEM. Lowest tritium accumulation was observed for samples exposed to D+Ar and D+Ne plasmas, which corresponds to the shallowest near surface damage zone, as confirmed by TEM.

1. Introduction

The main candidates for plasma-facing materials in fusion devices are currently tungsten and beryllium [1]. Tungsten has the advantage of a high sputtering threshold under hydrogen bombardment, good thermal conductivity and high melting point [2]. Properties of tungsten are sufficient for normal operations in current devices, however even tungsten will not be able to withstand excessive heat fluxes during off normal events such as ELM's without significant erosion or other damages (e.g. melting or cracking) in the future fusion devices. One of the options to mitigate excessive power loads is the divertor impurity plasma seeding for the energy dissipation. Gases like Ar, Ne or N can be used for that purpose. Many studies show a positive effect of gas puffing on spreading the energy over a large divertor or first wall area [3–6]. The presence of He as a reaction product from the DT fusion reaction is also unavoidable. All these impurities will have an effect on tungsten behavior under the plasma exposure. The expected impact of impurities on the surface morphology will change the tungsten erosion behavior. The presence of different subsurface defects created by the mixed plasma exposure will influence the retention of hydrogen isotopes [7,8], which is of prime importance for the operation of a fusion device. Moreover, the fuel trapping in the near surface damaged layer should not be neglected. Although many studies has been undertaken to understand the retention of tungsten exposed to mixed plasma, the detailed surface morphology studies correlated with fuel trapping are insufficient.

The main objective of this work is to determine the surface and subsurface morphology change of tungsten under low energy mixed plasma bombardment. The possible correlations of the morphology change and the tritium trapping in the material are investigated.

* Corresponding author.
E-mail address: m.rasinski@fz-juelich.de (M. Rasinski).

http://dx.doi.org/10.1016/j.nme.2016.11.001

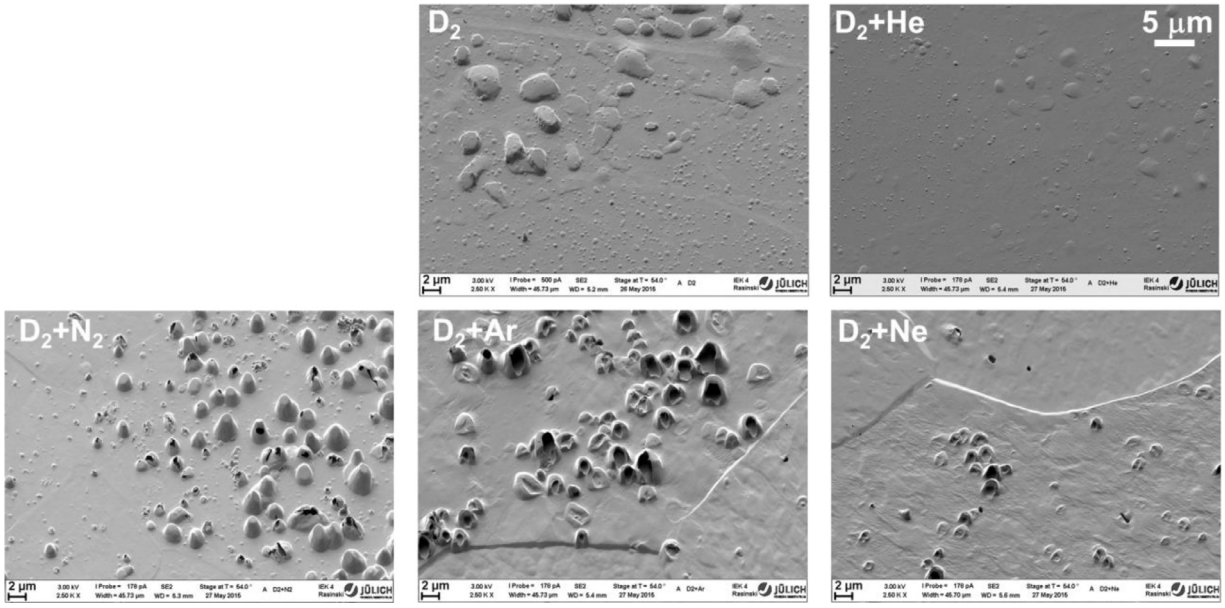

Fig. 1. Low magnification SEM images of the surface morphology of tungsten samples after plasma exposures.

2. Experimental

Tungsten samples provided by A.L.M.T. Corp., Japan were mechanically polished to obtain a mirror like surface and then recrystallized in vacuum at 1800 °C for 1 h. The recrystallization process was performed to limit the amount of existing defects in the samples and by that reduce the pre-existing H traps. Round samples with a surface diameter of 11 mm were pre-cut on the back side to split them in two parts after the exposure. Such prepared specimens were exposed in the linear plasma generator PSI-2 at a sample temperature of 500 K with an incident ion flux of about $10^{22}\,m^{-2}s^{-1}$ and an incident ion fluence of $5\times10^{25}\,m^{-2}$. Samples were biased to a potential of −100 V resulting in an incident ion energy of 70 eV. Details of the experimental setup on PSI-2 can be found elsewhere [9]. Samples were exposed to pure D^+ plasma and with additional impurities of He (3%), Ar (7%), Ne (10%) or N (5%). The impurity content was controlled by spectroscopy, except for N the content of which was estimated from puffing rates.

After the PSI-2 irradiation the samples were split into two pieces to conduct parallel post-mortem analyses. One piece of each exposed specimen was investigated to determine the microstructure modifications induced by different impurities in plasma. The surface morphology of the pristine tungsten and after the plasma exposure was analysed using a field emission scanning electron microscope (FE-SEM) Zeiss Crossbeam 540. A dual beam scanning electron microscope/focused ion beam (SEM/FIB) device, equipped with an electron backscattered diffraction (EBSD) detector was used for both surface imaging and grain orientation analysis. FIB was employed to prepare thin lamellas for the transmission electron (TEM) investigation in order to reveal the near surface damage zone. To minimize the influence of FIB preparation on defect creation two Pt protection layers were deposited, first starting with the electron beam deposition and subsequent ion beam deposition. TEM was conducted using field emission Tecnai G2 F20 microscope.

The second piece of each sample was transferred to Toyama University in order to perform a tritium loading. Before the tritium loading samples were outgassed at 573 K for 3 h in order to free traps from deuterium and to perform tritium loading. The loading was performed in a tritium-deuterium mixture with a tritium concentration of 7.1% and a pressure of 1.2 kPa at 573 K for 3 h. The tritium trapping in exposed samples was measured using the imaging plate (IP) technique. IP is a radiation image sensor based on the photo-stimulated luminescence, which is sensitive to low energy $\beta-$rays emitted by tritium from the sample. The range of $\beta-$rays from tritium in tungsten that can leave the surface and be analysed by IP is estimated to be ~300 nm [10]. That makes this technique very sensitive to the near surface fuel accumulation. This investigation method is widely used for tritium distribution measurements in fusion applications. Details of the technique and exemplary results can be find elsewhere [11–13].

3. Results and discussion

Figs. 1 and 2 illustrate the tungsten surface before and after plasma modification in low and high magnification, respectively. Exposure to pure D plasma leads to the formation of two types of blisters – small ones with a size of ~ 200 nm, homogeneously distributed on the surface and large ones with a size of few μm. The presence of larger blisters is strongly correlated with the tungsten grain orientation, which will be discussed further. Small blisters on top of large ones are also observed. A large number of small blisters are open. The general behaviour of various tungsten grains exposed to pure D plasma was in-detail described in [14].

Addition of He (3%) to deuterium plasma suppresses the blister formation visibly, which is also confirmed by other researchers [15]. The presence of both large and small blisters is visible, however the number of both blister types is lower. Moreover, large blisters are more flat when compared to blisters created at the tungsten surface exposed to pure D plasma. At high magnification, one can additionally notice a fine nano-sized structure present on the entire surface. That can be the effect of He nano-bubbles accumulated in the near-surface region, as described later. Addition of the N (5%), Ne (10%) or Ar (7%) leads to the formation of cone like shaped blisters, which appearance is, as for the previous case, correlated with the tungsten grain orientation. Moreover, on samples exposed to mixed plasma with Ne (10%) or Ar (7%), nearly all blisters are corrupted. This indicates that blisters appear relatively fast during the exposure and then are being eroded. A large fraction (but not all) of blisters is corrupted in the case of sample exposed to mixed plasma with N (5%). The difference in the behaviour should be attributed to a lower tungsten sputtering yield

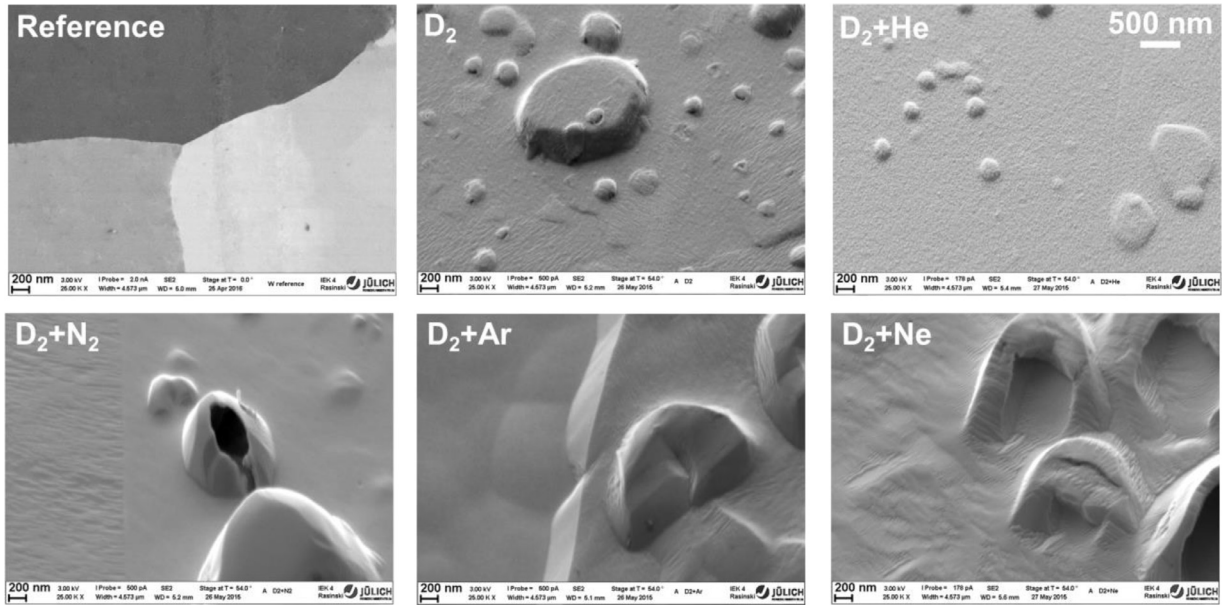

Fig. 2. High magnification SEM images of the surface morphology of tungsten samples in initial state and after plasma exposures.

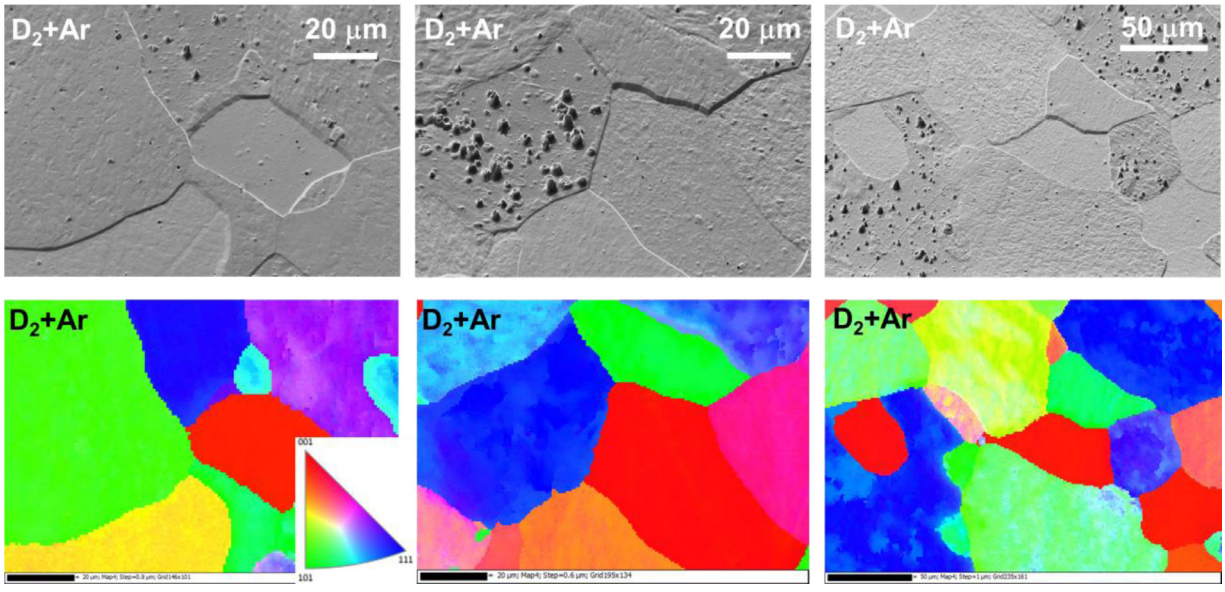

Fig. 3. SEM images with the corresponding IPF maps of the surface morphology of the sample exposed to D-Ar plasma. (For interpretation of the references to colour in the text, the reader is referred to the web version of this article.)

by N than by Ar and Ne. This can also be confirmed by the general sputtering behaviour of investigated samples. One can observe a distinct sputtering on the samples exposed to mixed plasma with Ne (10%) or Ar (7%) addition. The erosion is, moreover, strongly correlated with the tungsten grain orientation. To better understand the grain orientation effect on erosion, EBSD analysis of the sample exposed to D-Ar mixed plasma was performed. Fig. 3 illustrates the inverse pole figures (IPF) maps in the Z direction (perpendicular to the surface plane). Three random locations on the same sample are revealed. A clear relation between the grain orientation and both blister formation and erosion is visible. In all cases a pronounced blistering is observed on grains with orientation close to (111) – blue colour. The blistering behaviour should be attributed to the crystallographic orientation. For BCC metals, like tungsten, the preferred slip direction for plastic deformation is ⟨111⟩, which is perpendicular to the surface for grain oriented close to (111). In tungsten grains oriented close to (001) all four ⟨111⟩ directions are at shallow angle to the surface, which makes it less favourable for blistering to occur. This phenomenon is in the agreement with previous literature findings [16,17].

The highest local erosion is observed for grains with orientation close to (001) – red colour. The lowest erosion yield is observed for grains with orientation close to (101) – green colour. This finding is in contradiction to results reported by other groups [18] where most pronounce erosion was found to occur for grains oriented close to (101) and lowest erosion yield for grains with orientation close to (111). One has to notice, however, different irradiation conditions, namely energy of the impacting ions. In prior work [18] Ar ions with energy of 600 eV were used. If the different sputtering behaviour is true, it should than be assigned to a different energy of sputtering Ar ions – in this case the effect of grain orientation on sputtering would be energy dependent. More work

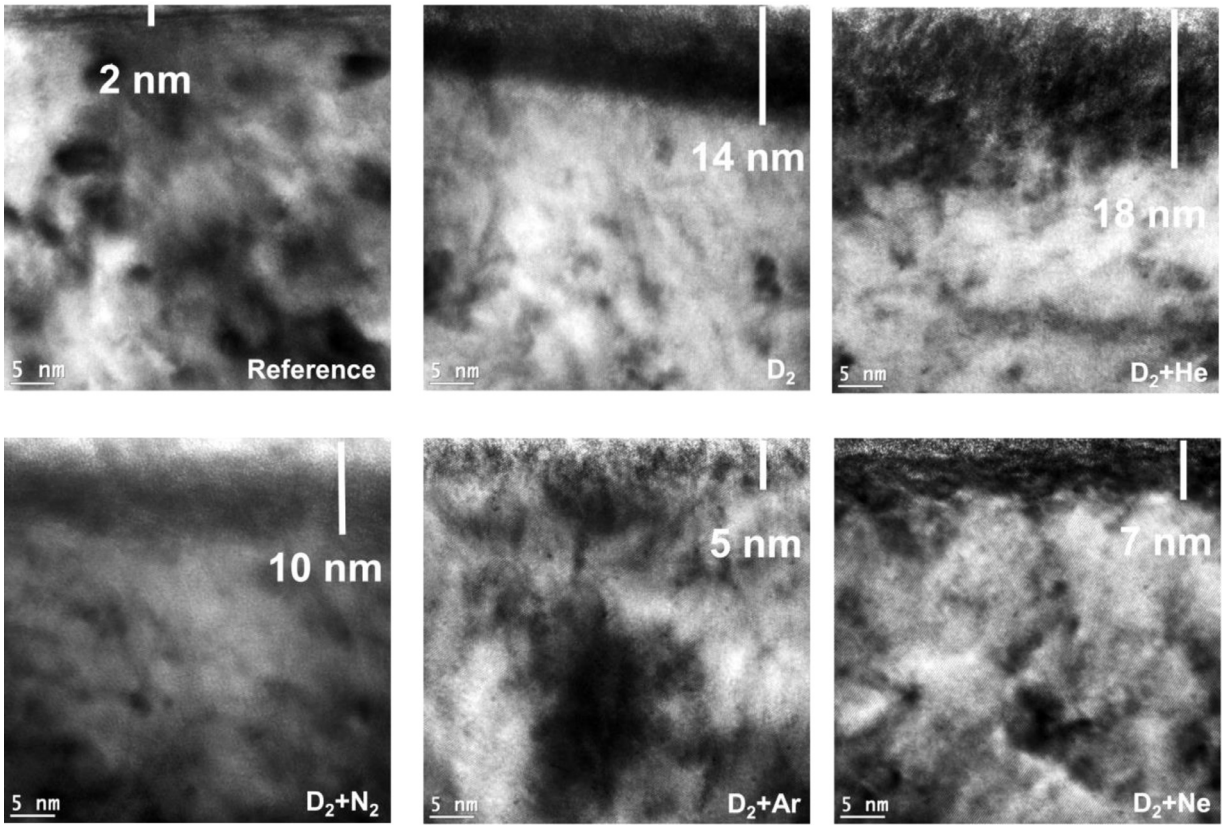

Fig. 4. TEM images of the cross-sections of the near surface layer of the sample in the initial state and after the plasma exposures.

is required to confirm that observation. For the samples exposed to D plasma, D+He and D+N mixed plasma it was impossible to perform EBSD investigation. The near surface damage zone was already too large and the EBSD signal was distorted. On the other hand there is no premise to believe that both blistering and erosion behaviour would be different from the analysed D+Ar sample.

Fig. 4 presents the TEM images of the cross-section of the pristine and exposed tungsten samples. The TEM investigation is focused on the very sub-surface region to determine the influence of plasma exposure on the near surface damage zone. In the pristine sample a very small damaged region (if any) with the thickness up to 2 nm can be detected. This type of damage can be attributed to sample preparation and handling. The largest damage zone, with a thickness of about 18 nm could be observed in the sample exposed to D+He mixed plasma. The lowest damage accumulation, with thicknesses of about 5 nm and 7 nm, was observed in the samples exposed to D+Ar and D+Ne plasmas, respectively. That can be explained by an accompanying erosion process that continuously removes the damages surface layer. On the samples exposed to D+N plasma, where erosion was less pronounced, created damage zone was larger, with a thickness of about 10 nm.

One has to remember that the measurements of damaged subsurface layer are very local and can vary depending on the location on the sample; however, the general trend described above should not differ distinctly.

The created damage zone has a strong impact on the subsequent tritium accumulation, as presented in Fig. 5. The highest uptake is reported for the sample exposed to mixed D+He plasma, which corresponds to the largest created near surface damage zone, as revealed by TEM. In the literature, it can be found that He addition decreases the D retention [8,15]. This fact should not be confused here. IP shows rather how many traps were created during the PSI-2 exposure in the near-surface layer of ~300 nm accessible by the technique. These traps are being filled with tritium during the loading process and the amount of stored tritium is visualized. The porous He induced structures (e.g. interconnected nano bubbles) can act as diffusion pathways for D back to the surface and thus reduce the D diffusion deeper in the bulk [19]. However, trap sites created in the near surface region could be easily occupied by post loaded T and revealed by the surface sensitive IP measurements. The lowest tritium uptake was reported for the samples exposed to mixed plasma with Ne (10%) or Ar (7%) addition. This is in good agreement with the TEM findings showing a shallow near surface damage zone. Additionally, assuming constant surface erosion, fewer defects should accumulate in the near surface layer. The tritium uptake in this case is comparable with the non-exposed, pristine sample. The effect of nitrogen seems to lie in-between He and Ar/Ne. Some additional defects are introduced by N (less than by He), but not sputtered away as efficiently as by Ar or Ne. Although TEM reveals a larger damage zone (14 nm) for the sample exposed to pure D plasma, a higher tritium uptake was observed for the sample exposed to mixed plasma with N (5%) addition. It should be correlated with the type and density of defects that are introduced in the near surface layer. Unfortunately the TEM investigation is not a technique that can distinguish and resolve all defects that can be present in the distorted structures (eg. single vacancies). . For that reason additional measurement as e.g. positron annihilation would be required. Similar observations of tritium trapping were found for tungsten exposed to pure He, N, Ar and D plasmas at a similar temperature and comparable ion energies [20]. The comparison of both experiments suggests that, for the mixed plasmas, the impurities and not the background deuterium ions are responsible for the formation and evolution of defects in tungsten.

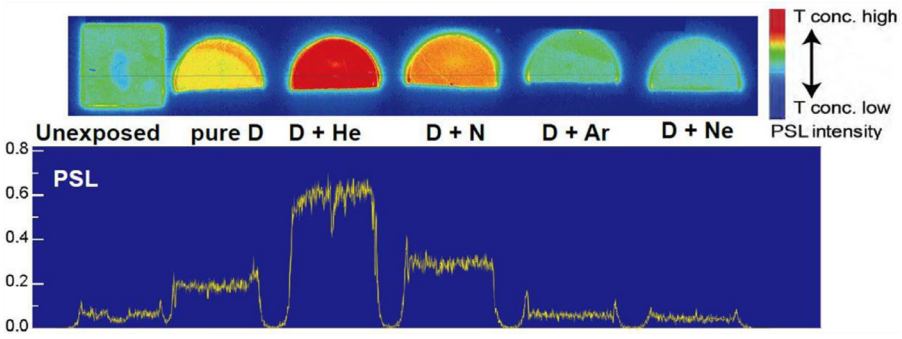

Fig. 5. Uptake of tritium in samples after plasma exposure and tritium loading, visualised by IP.

4. Conclusions

Polished and recrystallized tungsten samples were exposed in the linear plasma device PSI-2 to pure D plasma and with additional impurities of He (3%), Ar (7%), Ne (10%) or N (5%) at a temperature of 500 K and an incident ion energy of 70 eV.

The sample exposed to pure D+ plasma reveals the presence of two groups of blisters with a size of few μm and about 200 nm. The presence of blisters is strongly correlated with the tungsten grain orientation. Strongest blistering is reported for grains with orientation close to (111). The addition of Ar or Ne results in surface erosion with different yields depending on grain orientation. Highest erosion yield is observed for grains with orientation close to (100). Large blisters are present but show signatures of erosion. Less pronounced erosion is visible when adding N. The presence of N in the plasma causes also blisters with cone-like shapes. He addition leads to the formation of flatter blisters and a very fine nano-porosity on the surface.

The highest uptake of tritium was reported for the sample exposed to D+He plasma which corresponds to the largest – 18 nm, near surface damage zone revealed by TEM. Samples exposed to pure D and to D+N plasma had moderate tritium uptake. Addition of Ar or Ne to D plasma leads to no increase of tritium uptake when compared with the reference unexposed sample. These samples had also the smallest near surface damage zone.

Comparing the proposed seeding gases Ar, Ne and N, nitrogen is favourable with respect to the lowest erosion. However, erosion by Ar and Ne removes the defects in the material and leads to a lower tritium trapping.

Acknowledgement

This work has been carried out within the framework of the EUROfusion Consortium and has received funding from the Euratom research and training programme 2014–2018 under grant agreement No 633053. The views and opinions expressed herein do not necessarily reflect those of the European Commission.

References

[1] R.A. Pitts, et al., J. Nucl. Mater. 415 (2011) S957.
[2] M. Rieth, et al., J. Nucl. Mater. 432 (1-3) (2013) 482.
[3] A Kallenbach, et al., Plasma Phys. Control. Fusion 55 (2013) 124041.
[4] C. Giroud, et al., Nucl. Fusion 53 (2013) 113025.
[5] T. Nakano, et al., J. Nucl. Mater. 438 (2013) S291.
[6] I. Ivanova-Stanik, R. Zagórski, J. Nucl. Mater. 463 (2015) 596.
[7] H.T. Lee, et al., J. Nucl. Mater. 463 (2015) 974.
[8] M. Reinhart, et al., J. Nucl. Mater. 463 (2015) 1021.
[9] A. Kreter, et al., Fusion Sci. Technol. 68 (2015) 8.
[10] Y Hatano, et al., Phys. Scr. T167 (2016) 014009.
[11] Y. Torikai, et al., J. Nucl. Mater 438 (2013) S1121.
[12] T. Tanabe, et al., Fus. Sci. Technol. 41 (2002) 528.
[13] Y. Hatano, et al., J. Nucl. Mater. 463 (2015) 966.
[14] M. Balden, et al., J. Nucl. Mater. 452 (2014) 248.
[15] V Kh Alimov, et al., Phys. Scr. T138 (2009) 014048.
[16] WM Shu, et al., Phys. Scr. T128 (2007) 96.
[17] S Lindig, et al., Phys. Scr. T138 (2009) 014040.
[18] V.S. Voitsenya, et al., J. Nucl. Mater. 434 (2013) 375.
[19] M. Miyamoto, et al., J. Nucl. Mater. 415 (2011) S657.
[20] Y Hamaji, et al., Phys. Scr. T159 (2014) 014051.